



Mouse models of high-risk neuroblastoma

Alvin Kamili^{1,2} · Caroline Atkinson^{1,2} · Toby N. Trahair^{1,2,3} · Jamie I. Fletcher^{1,2}

Published online: 27 January 2020

© Springer Science+Business Media, LLC, part of Springer Nature 2020

Abstract

Informative and realistic mouse models of high-risk neuroblastoma are central to understanding mechanisms of tumour initiation, progression, and metastasis. They also play vital roles in validating tumour drivers and drug targets, as platforms for assessment of new therapies and in the generation of drug sensitivity data that can inform treatment decisions for individual patients. This review will describe genetically engineered mouse models of specific subsets of high-risk neuroblastoma, the development of patient-derived xenograft models that more broadly represent the diversity and heterogeneity of the disease, and models of primary and metastatic disease. We discuss the research applications, advantages, and limitations of each model type, the importance of model repositories and data standards for supporting reproducible, high-quality research, and potential future directions for neuroblastoma mouse models.

Keywords Neuroblastoma · GEMM · PDX · Mouse model · Pre-clinical testing

1 Introduction

Neuroblastoma is a tumour of infancy and early childhood [1] that arises from neural crest progenitors that aberrantly persist during sympathetic nervous system development [2]. High-risk disease is associated with amplification of the *MYCN* oncogene, which occurs in > 30% of high-risk tumours [3], and recurrent patterns of whole-chromosome or large segmental DNA copy number alterations, which occur in almost all high-risk neuroblastomas [1]. Comprehensive genomic landscape studies demonstrate that paediatric cancers, including neuroblastoma, have lower mutation rates than adult cancers [3–5]. Furthermore, in paediatric cancers, frequently mutated driver genes typically occur in a mutually exclusive manner, in contrast to adult cancers where co-mutation of multiple driver genes is more common [4]. These differences reflect the distinct origins of paediatric and adult tumours, with the former

arising over short time periods during development and the latter a consequence of accumulated changes over longer timeframes. These observations may have direct consequences for therapy, with single, truncal driver mutations being ideal therapeutic targets. Single, potent cancer drivers are also well-suited to modelling with genetically engineered mouse models (GEMMs). GEMMs have consequently played a major role in the experimental validation of *MYCN* amplification [6], *ALK* mutation [7–9], and *LIN28B* overexpression [10] as drivers of neuroblastoma tumorigenesis and in assessing the contribution of a range of cancer-associated genes with malignant transformation, tumour growth, and metastasis. Neuroblastoma GEMMs have also been used to characterize a range of drug resistance genes, validate drug targets, and as pre-clinical testing models for the initial assessment of novel therapeutics including immunotherapies. In contrast to GEMM models, patient-derived xenografts (PDXs) developed directly from tumour specimens allow biology and pre-clinical testing studies that are more representative of the diversity of high-risk neuroblastomas, allow for the study of metastatic disease, facilitate modelling of more complex potential drivers that are challenging for GEMM strategies, and provide opportunities to refine personalized therapy recommendations for neuroblastoma patients. Here, we review current mouse models of neuroblastoma and their diverse applications, focusing on GEMM and PDX models.

✉ Jamie I. Fletcher
jfletcher@ccia.org.au

¹ Children's Cancer Institute Australia, Lowy Cancer Research Centre, UNSW Sydney, Kensington, NSW, Australia

² School of Women's and Children's Health, UNSW Sydney, Kensington, NSW, Australia

³ Kids Cancer Centre, Sydney Children's Hospital, Randwick, NSW, Australia

2 Genetically engineered mouse models: understanding disease and validating drivers

2.1 GEMMs of *MYCN*-amplified high-risk neuroblastoma

The Th-*MYCN* transgenic mouse model, developed in 1997 [6], is the most widely used and best characterized of the neuroblastoma GEMMs. In this model, human *MYCN* expression is targeted to developing neuroblasts under control of a rat tyrosine hydroxylase (Th) promoter. Mice homozygous for the *MYCN* transgene spontaneously develop neuroblastoma, which arises from highly proliferative Phox2B-positive neuronal progenitors in early postnatal sympathetic ganglia [6, 11, 12]. Whereas neuroblasts in the ganglia undergo hyperplasia and complete regression within 2 weeks of birth in normal mice, *MYCN* transgene expression increases hyperplasia, delays regression, and allows the persistence of neuroblasts from which the tumour arises [11]. This process likely parallels the neuroblast hyperplasia observed in the adrenal medulla of infants, which is observed at a 40 times higher incidence than clinical neuroblastoma [2, 13]. Tumour incidence varies substantially with mouse background but can reach 100% in some genetic backgrounds [14, 15] (Table 1). Th-*MYCN* tumours recapitulate the histopathology of the human disease [6], and comparative genomic hybridization and copy number analyses reveal that the mouse tumours can harbour copy number alterations in regions syntenic to those commonly altered in human neuroblastoma. These include gain of the mouse orthologue of chromosome 17q and further amplification of the *MYCN* transgene [14, 15, 17]. Th-*MYCN* mice homozygous for the transgene have a short latency of 4–7 weeks to tumour formation on a 129X1/SvJ background, and a short time from palpable tumour to sacrifice, averaging only 5 days [14]. Hemizygous mice develop tumours at significantly lower incidence and longer latency [14, 15]. Microscopic metastases can be observed in a range of organs, but are not typically present in bone or bone marrow [6, 18].

Th-*MYCN* tumours have been successfully imaged using a range of clinically relevant imaging modalities, including magnetic resonance imaging (MRI) [19, 20], ultrasound [19], positron emission tomography (PET) [21], and ¹³¹I-metaiodobenzylguanidine (MIBG) scintigraphy [22]. Bioluminescence imaging has also been achieved by crossing the Th-*MYCN* model with E₂F₁-luciferase mice [23].

A more recently developed transgenic model of *MYCN*-amplified neuroblastoma, the LSL-*MYCN*;Dbh-iCre mouse [16], allows conditional expression of *MYCN* in dopamine β-hydroxylase (*Dbh*) expressing cells. In this model, tumours arise in the postnatal sympathetic ganglia and adrenal medulla. As with Th-*MYCN* mice copy number, gains and losses in regions syntenic to those commonly altered in human neuroblastoma are observed, including gain of the mouse orthologue of chromosome 17q and *MYCN* transgene amplification [16]. While time to tumour development in the LSL-*MYCN*;Dbh-iCre model is much more variable and substantially longer (80 days on average) than that of the Th-*MYCN* model (Table 1), tumour incidence remains relatively high on a range of genetic backgrounds, which is an advantage when crossing these mice with other GEMM models.

2.2 GEMMs of *ALK*-mutant neuroblastoma

Gain-of-function germline *ALK* mutations are found in the majority of familial neuroblastomas [24, 25] and 8–9% of sporadic high-risk neuroblastomas at diagnosis, where it is the most frequently somatically mutated gene [3, 26]. GEMM models have been described for the two most frequently occurring activating mutations, *ALK*^{R1275} (43%) and *ALK*^{F1174} (30%) [26]. Dbh-iCre/CAG-LSL-*ALK*^{F1174L} mice and Th-IRES-Cre/CAG-LSL-*ALK*^{F1174L} mice [7] which express the *ALK* mutant in Dbh- or Th-positive neural crest tissues respectively give rise to neuroblastoma with a penetrance < 50% and very long latency of 130–351 days, with tumours arising in paravertebral ganglia or adrenal gland, with extensive liver metastases in some mice [7] (Table 1). As with

Table 1 GEMM models of high-risk neuroblastoma

GEMM	Aberration modelled	Tumour incidence ¹	Average tumour latency ¹	Reference
Th- <i>MYCN</i>	<i>MYCN</i> amplification	5–100%	4–7 weeks	[6]
LSL- <i>MYCN</i> ;Dbh-iCre	<i>MYCN</i> amplification	> 75%	80 days	[16]
Dbh-iCre/CAG-LSL- <i>ALK</i> ^{F1174L}	<i>ALK</i> mutation	< 50%	130–351 days	[7]
Th-IRES-Cre/CAG-LSL- <i>ALK</i> ^{F1174L}	<i>ALK</i> mutation	0% ²	NA	[8]
Th- <i>ALK</i> ^{F1174L}	<i>ALK</i> mutation	0% ²	NA	[9]
<i>ALK</i> ^{R1275Q} knock-in	<i>ALK</i> mutation	25%	56 days	[10]
Dbh-iCre/CAG-LSL- <i>Lin28b</i>	LIN28B overexpression			

¹ Tumour incidence and latency varies between mouse backgrounds. ² The Th-*ALK*^{F1174L} and *ALK*^{R1275Q} knock-in models do not form spontaneous tumours but cooperate with *MYCN* to accelerate tumour formation when crossed with Th-*MYCN* mice

other neuroblastoma GEMMs, chromosomal aberrations syntenic to those of the human disease were observed; however, the number of aberrations is significantly higher than in models of *MYCN*-amplified disease [7, 27], consistent with the hypothesis that *ALK* mutation alone is not sufficient for tumorigenesis and that secondary hits are required for neuroblastoma development. When Dbh-iCre/CAG-LSL-*ALK*^{F1174L} mice were crossed with Th-*MYCN* mice, the resulting progeny had markedly higher tumour incidence and substantially shortened tumour latency, and the resulting tumours had very few genomic aberrations [7, 27]. A second *ALK*^{F1174L} mouse model, Th-*ALK*^{F1174L} [8], did not form spontaneous tumours; however, when crossed with Th-*MYCN* mice, the resulting double transgenic mice had substantially increased tumour incidence and decrease latency compared to Th-*MYCN* mice on the same background, with tumours arising in both paraspinal ganglia or adrenal glands [8] (Table 1). Similarly, an *ALK*^{R1275Q} knock-in mouse crossed with Th-*MYCN* mice on a 129 × B6 genetic background had complete tumour penetrance, whereas neither the *ALK*^{R1275Q} knock-in mice or Th-*MYCN* mice developed tumours on this background [9] (Table 1).

2.3 LIN28B transgenic mice

The RNA-binding protein LIN28B is a negative regulator of let-7 siRNA family [28], which in turn function as tumour suppressors by negative regulation of *MYCN* [29]. *LIN28B* polymorphisms that cause elevated LIN28B protein expression are highly associated with the risk of developing of high-risk neuroblastoma [30]. Conversely, LIN28B overexpression is observed in the majority of high-risk neuroblastomas, with *LIN28B* amplification also occurring in a small percentage of tumours [10]. Conditional *Lin28b* transgenic mice (Dbh-iCre/CAG-LSL-*Lin28b* mice) develop spontaneous neuroblastoma with tumour incidence of 25% [10] and a short latency [27], with tumours arising in ganglia and adrenal glands [10] (Table 1). *Lin28b* transgenic tumours have fewer additional genomic events than GEMMs modelling *MYCN* amplification or *ALK* mutation, with event numbers closer to that of a Th-*MYCN-ALK*^{F1174L} double transgenic [27], suggesting that *LIN28B* aberrations are strongly oncogenic.

2.4 Validating cancer-associated genes in neuroblastoma GEMMs

Neuroblastoma GEMM models, particularly the Th-*MYCN* mouse, have been utilized extensively to genetically dissect the role of cancer-associated genes in neuroblastoma tumorigenesis, metastasis, and drug resistance. Tumorigenesis in this model is accelerated by clinically relevant aberrations in a range of tumour suppressor or putative tumour suppressor genes and by activation of

other oncogenes. Conversely, tumour formation is delayed, or the incidence of tumour formation reduced, by loss of several other putative oncogenes (Table 2).

As discussed above, the most common activating *ALK* mutations found in spontaneous human neuroblastoma, *ALK*^{R1275} and *ALK*^{F1174} [26], shorten the latency and increase tumour penetrance in the Th-*MYCN* mouse [7–9]. Decreased latency and increased tumour incidence are also observed with loss of Neurofibromin 1 (*Nf1*) [6] in this model. Loss of *NF1* and other aberrations activating the RAS-MAPK signalling pathway are relatively rare in high-risk neuroblastoma at diagnosis, however are highly enriched at relapse and also include activating mutations of *PTPN11*, *NRAS*, *HRAS*, *BRAF*, and *FGFR1* [3, 32, 35]. Loss of the tumour suppressor *Tp53* in the Th-*MYCN* model also shortens latency and increases tumour penetrance [23]. Conversely, targeted deletion of the p53 E3 ubiquitin ligase MDM2 Proto-Oncogene (*Mdm2*) leads to p53 stabilization, delays tumour formation, and decreases tumour incidence in the Th-*MYCN* model [44]. Notably, compensatory silencing of *Ink4a/Arf* (alternate reading frame of *Cdkn2a*), a negative regulator of *Mdm2* is observed in mice with heterozygous *Mdm2* loss [44]. In human neuroblastoma, loss of p53 function is rare at diagnosis but common in post-treatment and relapsed tumours and strongly associated with drug resistance. Loss of p53 function occurs through multiple nodes of the p53 activation pathway, including by *TP53* mutation, *MDM2* amplification, and inactivation of *INK4a/ARF* [32–34]. Loss or loss of function of other established tumour suppressors, including the RB transcriptional corepressor 1 (*Rb1*) [6] and Clusterin (*Clu*) [37] also accelerate tumorigenesis or increased tumour incidence in the Th-*MYCN* model, while delayed tumorigenesis and decreased tumour incidence are observed with deletion of the cytokine/growth factor Midkine (*Mdk*) [45] or Caspase 2 (*Casp2*) [47]. While expression of extracellular and cytoplasmic clusterin is associated with differentiated or localized neuroblastoma [37] and plasma midkine strongly associated with poor prognosis [46], *RB1* and *CASP2* aberrations are rarely if ever observed in the human disease [36, 47].

Despite the spontaneous development of neuroblastoma at clinically relevant anatomic sites in the Th-*MYCN* mouse model, metastatic spread is limited to micrometastases in a broad range of organs, with bulky metastases rarely observed. Bone and bone marrow metastases are particularly uncommon in this model, and limited to micro-metastatic disease [6, 18, 38]. As *CASP8* is frequently inactivated in high-risk neuroblastoma [39, 40] and *CASP8* loss increases the metastatic phenotype *in vitro* [41], Teitz et al. crossed the Th-*MYCN* mice with conditional *Casp8* knockout mice. The resulting progeny had a substantially increased incidence of bone marrow metastasis, increased from 5 to 37%, without impacting the growth of the primary tumour [38]. Increased metastasis is also observed in mice transgenic for both *MYCN* and *MYCNOS*, the cis-antisense gene of *MYCN* (alternatively

Table 2 Genes modifying tumorigenesis, metastasis, and drug resistance in the Th-*MYCN* mouse model

Modifier gene in Th- <i>MYCN</i> mouse	Correlate in human neuroblastoma	Mouse phenotype
Tumour suppressor loss		
<i>Tp53</i> deletion [23, 31]	Loss of p53 function through <i>TP53</i> mutation, <i>MDM2</i> amplification, and INK4a/ARF inactivation is common in post-treatment and relapsed high-risk neuroblastoma [32–34].	Accelerated tumorigenesis, increased tumour incidence, resistance to ionizing radiation and cyclophosphamide
<i>Nf1</i> loss of function [6]	<i>NF1</i> loss, and other aberrations activation RAS-MAPK signalling are recurrent at diagnosis and highly enriched at relapse [3, 32, 35].	Accelerated tumorigenesis and/or increased tumour incidence
<i>Rb1</i> loss of function [6]	Rarely observed in neuroblastoma [36].	
<i>Clu</i> deletion [37]	Expression of extracellular and cytoplasmic clusterin is associated with differentiated or localized neuroblastoma [37].	
<i>Casp8</i> loss [38]	<i>CASP8</i> is frequently inactivated in neuroblastoma [39, 40] and increases metastatic phenotype <i>in vitro</i> [41].	Increased metastasis
Oncogene activation		
<i>ALK</i> activating mutations [7–9]	Activating <i>ALK</i> mutations are a driver of familial neuroblastoma [24, 25], recurrent at diagnosis [3, 26] and significantly enriched at relapse [42].	Accelerated tumorigenesis and/or increased tumour incidence
<i>MYCNOS</i> expression [43]	Cis-antisense gene of <i>MYCN</i> (<i>MYCNOS</i>) co-amplified and co-expressed with <i>MYCN</i> and associated with poor prognosis [43]	Increased metastasis
Oncogene deletion		
<i>Mdm2</i> deletion [44]	Loss of p53 function through <i>MDM2</i> amplification and p14(ARF) inactivation is common in high-risk neuroblastoma [33].	Delayed tumorigenesis and/or decreased tumour incidence
<i>Mdk</i> deletion [45]	Plasma midkine strongly associated with poor prognosis [46].	
<i>Casp2</i> [47]	Novel finding.	
<i>Abcc1</i> deletion [48, 49]	<i>ABCC1</i> expression associated with poor survival [50].	Delayed tumorigenesis, resistance to vincristine and etoposide
<i>Abcc4</i> deletion [51]	<i>ABCC4</i> expression associated with poor survival [52].	Resistance to irinotecan

known as *NCYM*) [43], although metastasis to bone and bone marrow is not observed. *MYCNOS* is normally co-amplified and co-expressed with *MYCN* and inhibits GSK3 β activity, thus stabilizing the *MYCN* protein. Interestingly, transgenic mice for only *MYCNOS* did not develop neuroblastoma and *MYCN-MYCNOS* double transgenic mice developed tumours at the same rate as *MYCN* single transgenic mice [43].

The Th-*MYCN* model has also been used to assess the contribution of cancer-associated genes to therapy resistance. As mentioned above, loss of p53 function is uncommon at diagnosis, but is frequently observed at post-treatment, and is associated with chemoresistance. *Tp53* loss in the Th-*MYCN* mouse confers resistance to cyclophosphamide [23] and ionizing radiation [31], in part through metabolic adaptations. Beyond p53, the multidrug resistance proteins *ABCC1* and *ABCC4* are *MYCN* target genes are associated with neuroblastoma outcomes [50, 52] and are capable of conferring resistance to a range of conventional chemotherapies used in induction and salvage therapy for high-risk disease. Loss of

Abcc1 in the Th-*MYCN* mouse sensitizes allografts to etoposide and vincristine [48] and loss of *Abcc4* sensitizes Th-*MYCN* mouse tumours to irinotecan [51].

2.5 Neuroblastoma GEMMs as models for pre-clinical testing

The high degree of similarity to human neuroblastoma, spontaneous development in appropriate tissues, high tumour incidence, and short latency of the Th-*MYCN* model make it an attractive and practical model for pre-clinical testing studies, particularly for therapeutics directly or indirectly targeting *MYCN* or pathways associated with *MYCN* amplification. Tumour monitoring is also tractable in this model using a wide range of imaging modalities, including those used clinically [19–23] (Section 2.1).

Concordant with most *MYCN*-amplified high-risk human tumours at diagnosis, Th-*MYCN* mouse tumours respond to standard-of-care induction therapy agents, including

cyclophosphamide, vincristine, etoposide, cisplatin, and irinotecan [23, 48, 51, 53, 54], as well as to standard salvage regimens of cyclophosphamide/topotecan and irinotecan/temozolomide [54–56]. Models of drug resistant neuroblastoma have also been established that mirror the human disease. Th-*MYCN*/*Tp53*^{+/-} mice are more resistant to cyclophosphamide [23], while Th-*MYCN* mice with a tamoxifen-inducible p53ER^{TAM} fusion protein expressed from a knock-in allele (Th-*MYCN*/*Tp53*^{KI/KI} mice) are resistant to ionizing radiation [31]. Repeated exposure to cyclophosphamide has also been used to develop Th-*MYCN* tumours with intrinsic chemoresistance and a propensity for bone marrow metastasis, thus more faithfully representing relapsed or chemo-refractory disease [57] and demonstrating that this model might be useful for identifying drug resistance mechanisms.

As a pre-clinical testing model, the Th-*MYCN* model has been extensively used to assess novel small molecule inhibitors targeting angiogenesis [18], the polyamine pathway [53, 55, 56], multidrug transporters [48], histone deacetylases [58, 59], Aurora kinases [60, 61], Bromodomain and extra terminal (BET) family adaptor proteins [62], the histone chaperone FACT [54], cyclin-dependent kinases [63], and PA2G4, a novel regulator of *MYCN* stability [64], amongst numerous other examples [65, 66]. In many of these examples, pre-clinical activity is also observed in xenograft models of high-risk neuroblastoma, suggesting that activity is not simply attributable to the use of a homogeneous and chemo-naïve model with dependence on a single oncogene.

A major advantage of GEMM systems for pre-clinical testing is the development of tumours in an immune-competent host, allowing assessment of immunotherapies, and more informative assessment of conventional agents, many of which stimulate tumour-specific immune responses [67]. In addition to GEMM models of neuroblastoma, transplantable cell line models derived from the Th-*MYCN* mouse on a C57Bl/6 background allow transplantation into syngeneic hosts [68]. These models have allowed testing combinations with standard-of-care GD2 MAb immunotherapy [69] and with checkpoint inhibitors [70] and are likely to play a significant role in further development of immunotherapy approaches.

3 Patient-derived xenograft models of high-risk neuroblastoma

3.1 Modelling of the diversity of high-risk neuroblastoma

While GEMM models have contributed enormously to our understanding of neuroblastoma tumorigenesis, progression and response to therapy, particularly with respect

to the roles of *MYCN* amplification and *ALK* mutation, they do not fully reflect the diversity of the human disease, and indeed different high-risk neuroblastoma modelling approaches have different strengths and weaknesses for various applications (Table 3). Neuroblastoma is often described as copy-number-driven cancer [1], with loss of chromosome 1p, 11q and gain of chromosome 17q being both recurrent and strongly associated with poor outcome [12]. *TERT* rearrangements also occur in 25% of high-risk neuroblastomas and are associated with very poor prognosis [13, 14]. Modelling these more complex potential drivers is considerably more challenging and while such models might potentially be developed using contemporary genome editing techniques [15, 17], no neuroblastoma GEMMs exist for these aberrations to date. Furthermore, the diversity of potential high-risk neuroblastoma drivers and potential drug targets that occur recurrently at low frequency [3, 32, 34] makes comprehensive modelling using GEMM strategies impractical.

In contrast, PDX models developed directly from patient tumour materials and subsequently maintained by direct animal to animal passage allow more comprehensive representation of the diversity of high-risk neuroblastomas and provide opportunities to refine personalized therapy recommendations for neuroblastoma patients. PDX models are generally considered to more closely represent human cancers than xenografts from established cell lines, since the tumour material is not compromised by *in vitro* adaptation, which can include acquisition of new genetic aberrations [71]. PDX tumour models typically retain histologic and molecular heterogeneity characteristic of the originating patient tumour [72–75] and at least in the short term can maintain aspects of the tumour architecture and microenvironment if transplanted as tissue fragments [75, 76]. For these reasons, PDX models are widely considered to provide a realistic pre-clinical platform for assessing new treatments with a high probability of success when translated to patients [71, 76, 77].

Early attempts of neuroblastoma xenografting were reported in the 1980s and assessed tumour growth following chemotherapy and surgery [78] and the relationship between PDX growth rate, drug sensitivity and expression of tumour-specific markers [79]. Engraftment of a large cohort of 58 neuroblastoma tumours was reported in 1993 and established a correlation between engraftment potential and patient treatment outcome [80]. Following these early studies there was a paucity of model development for many years in favour of the technical and economical simplicity of cell culture. However, given the limited translational potential of results obtained from *in vitro* cell cultures [81], PDX models are increasingly being established as a highly valuable tool in drug development, pre-clinical testing and personalized medicine [82]

Table 3 Benefits and disadvantages of model types

	GEMM models		PDX models	
	Advantages	Disadvantages	Advantages	Disadvantages
Tumorigenesis studies	<ul style="list-style-type: none"> • Spontaneous tumour development allows study of primary tumour initiation • Allows interrogation of the role of genes in tumour initiation • Potential for forward genetic screens 	<ul style="list-style-type: none"> • Difficult to model common high-risk neuroblastoma aberrations, such as segmental chromosomal gains and losses, chromothripsis • Limited scope to study mechanisms of tumour metastasis 	<ul style="list-style-type: none"> • Ability to model spontaneous and experimental metastasis (as orthotopic models) 	<ul style="list-style-type: none"> • Primary tumour development is bypassed
Pre-clinical testing studies	<ul style="list-style-type: none"> • Well-characterized models of <i>MYCN</i>-amplified, <i>ALK</i>-mutant, and <i>TP53</i>-deficient neuroblastoma available • Immune-competent host allows testing of immunotherapies • Tumours maintain native stroma and vasculature • Tumours arise at anatomically relevant sites • Clinically relevant imaging modalities are effective 	<ul style="list-style-type: none"> • Limited availability of models representing commonly altered drug targets or pathways • Limited scope to study response in metastatic disease • Most models represent chemonaïve disease • Drug targets are murine 	<ul style="list-style-type: none"> • Representative of the diversity of the patient population • Large numbers of models available internationally • Potential for patient-specific modelling and direct comparisons to patient outcomes (early passage) • Drug targets are human • Can model response to both primary and metastatic disease • Clinically relevant imaging modalities are effective 	<ul style="list-style-type: none"> • Immune-deficient host, currently limited scope for immune reconstitution • Tumour stroma and vasculature are different species

(Fig. 1) and several new cohorts of neuroblastoma models have recently been reported [83, 84].

3.2 Methodologies for PDX development

Heterotopic neuroblastoma PDX models are typically established as subcutaneous xenografts, while orthotopic neuroblastoma models are typically established in the mouse adrenal [83–85] (see Section 3.3). Neuroblastoma xenografts have successfully been established from a range of patient biomaterials, including primary and metastatic solid tumour samples, bone marrow, peripheral blood, fluids drained from malignant ascites, pleural effusions, and residual cells from routine cytogenetics analysis [83–85]. Patient tumour materials that contain a substantial number of T-lymphocytes, such as bone marrow, pleural fluid, and lymph node samples, may require lymphocyte depletion prior inoculation to avoid graft *versus* host disease in recipient mice [84, 86]. Additionally, the presence of B lymphocyte populations in samples such as lymph node or pleural fluid may cause development of EBV-associated atypical B-lymphoma proliferation in highly immune-deficient strains [84, 87–89], with incidence in NOD/SCID/IL2 γ -receptor null (NSG) mice reported to be as high as 32% [87].

We recently reported higher engraftment success for samples from patients at relapse (100% from 6 samples) than for those from patients at diagnosis (31% from 13 samples) [84], consistent with other studies that reported 33% at relapse and of 24% at diagnosis [83] or 45% from INSS stage IV disease with an association between patient outcome and engraftment success [80]. Engraftment times are frequently long however, with previous studies reporting a range of 2 to 10 months [90], 2.5 to 10 months [83], and 1 to 7 months [84]. A range of approaches may improve engraftment rate and decrease engraftment time. While BALB/C nude, SCID, and NOD/SCID strains have all successfully be used to establish neuroblastoma xenografts, NOD/SCID/IL2 γ -receptor null (NSG) mice are now commonly utilized and have superior success rates than other models [82]. Using head-to-head comparisons, orthotopic adrenal inoculation has recently been shown to result in more rapid and reliable engraftment than either subcutaneous or intramuscular sites, despite high concordance between tumours from each site based on histology and copy number analyses [84]. While the reasons for more rapid orthotopic engraftment are unclear, the adrenal gland is the most common site of origin for primary neuroblastoma [1] and previous studies have suggested that non-subcutaneous sites may provide greater protection of the engrafted cells against hypothermic insult [91], or a greater capacity for angiogenesis [90, 92, 93]. PDX model engraftment success is influenced by many other factors, including the viability and cellularity of the donor sample, time from biopsy to inoculation, patient treatment status at tissue collection, and sample type [82, 94]. Given the central role of the microenvironment

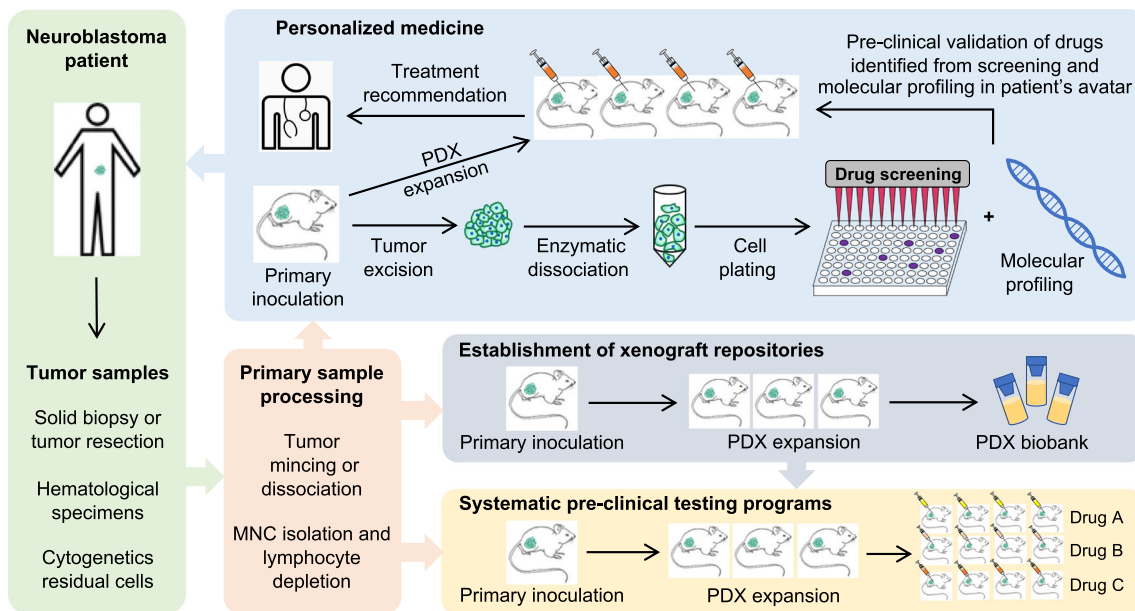


Fig. 1 Patient-derived xenograft (PDX) models of high-risk neuroblastoma in translational research and personalized medicine. Tumour samples for xenografting can be obtained from tumour biopsy, resection, haematological samples, or cytogenetics residual cells and processed for primary inoculation by mincing the tumour into smaller pieces or isolating mononuclear cells (MNC) from haematological samples followed by lymphocyte depletion. Upon establishment and expansion, xenograft

tissues can be banked as renewable source of research materials, and along with other newly established models can be used as a platform for systematic pre-clinical testing of novel anticancer drugs. PDX models can also play a key role in personalized medicine by providing material for unbiased *ex vivo* drug sensitivity screening and avatar-based pre-clinical testing to inform individualized patient therapy

in tumour biology and the presence of tumour-associated macrophages, fibroblasts, pericytes, endothelial cells, and extracellular matrix in neuroblastoma xenografts [95], maintaining tumour cell interactions as mouse components replace these cellular components may also improve engraftment. Matrigel is often used to increase engraftment efficiency; however, emerging approaches that mimic biological scaffolds, such as graphene-based nanomaterials [96], functionalized scaffolds [97], and biodegradable matrices [98], may provide new opportunities to increase engraftment efficiency.

3.3 Orthotopic PDX model development

Orthotopic models of neuroblastoma are typically established directly in the mouse adrenal gland [92], thus modelling the most common site of human neuroblastoma development [1]. While in general orthotopic models are more labour intensive to establish, they have been reported to be more similar to donor tumours based on histology and gene expression levels and to better predict patient tumour progression and response to treatment [94, 99]. As mentioned above, orthotopic implantation of high-risk neuroblastoma samples may also increase the likelihood of developing a patient-specific models within a clinically useful timeframe [84]. Surgical establishment of adrenal xenografts involves exposing the adrenal gland and injection of cells through the adrenal fat pad into the adrenal gland [92], or placement of intact tumour fragments in the para-adrenal space [95]. Alternatively, ultrasound-guided injection of cells into the

adrenal or para-adrenal space has been described as less invasive procedure [19]. Here, a catheter is inserted into anaesthetised mice through the skin, and guided by ultrasound, a needle with syringe containing cell suspension is inserted through the catheter and into the space between the kidney and adrenal gland or into the adrenal capsule [19].

Orthotopic models demonstrate growth and dissemination of neuroblastoma cells similar to that observed in high-risk neuroblastoma patients. Numerous studies report spontaneous metastasis to clinically relevant sites such as liver, spleen, and lymph nodes [100], with other studies showing dissemination to bone and bone marrow [90, 92]. Further, metastatic patterns appeared similar to patients with particular genomic features, such as a high frequency of liver metastases as seen in *MYCN*-amplified high-risk patients [101]. Importantly, orthotopic tumours retain histopathological features such as robust expression of synaptophysin and chromogranin, preserve subcellular features of primary patient tumours such as dense core vesicles and gene expression and DNA methylation profile of patients' tumours [90, 100]. Orthotopic tumours have also been reported to show increased proliferation, invasion, chemosensitivity, and angiogenesis [92, 101, 102] in comparison to subcutaneous models.

While monitoring tumour progression is less straight forward for orthotopic models, a range of clinically relevant imaging modalities are suitable for monitoring PDX tumours, as for GEMM models (see Section 2.1) and stable incorporation of reporters for bioluminescence and fluorescence is well established in xenograft models [103–105].

3.4 Xenograft models of metastatic neuroblastoma

While GEMMs and PDXs provide excellent and diverse models of primary neuroblastoma tumours, modelling of metastatic neuroblastoma is less commonly attempted, despite the clinical imperative for new treatments for metastatic disease, the presence of widespread metastasis as a defining feature of high-risk neuroblastoma [1] and the possibility that neuroblastoma relapse arises from disseminated clones present at diagnosis [106]. Common sites of high-risk neuroblastoma metastases include bone (55% of patients with metastatic disease), bone marrow (80%), liver (30%), lymph nodes (30%), and central nervous system (CNS, 5%) [107–109].

A range of approaches have been applied to modelling metastatic neuroblastoma, including spontaneous metastasis models where metastases arise stochastically from a xenografted primary tumour, thus modelling the entire metastatic process; experimental metastasis models where tumour cells are delivered intravenously, thus bypassing the steps of tumour invasion and intravasation; and direct injection models where tumour cells are engrafted directly in the site of interest. Orthotopic neuroblastoma xenografts have been reported to spontaneously metastasize to clinically relevant sites including as bone marrow, liver, and lymph nodes [92, 101, 103, 105, 110]. While the post-mortem identification of microscopic metastases is labour intensive [111], this process is considerably simplified by incorporating reporter genes allowing bioluminescence or fluorescence, and the technical issue of intense primary tumour signal limiting the ability to accurately detect metastases [105] can be overcome by surgical resection of the primary tumour [112, 113]. This approach also allows the further growth of micrometastases in mice that would have reached ethical endpoints based on primary tumour size. For experimental metastasis models, intravenous (tail vein) delivery of tumour cells is a commonly used, leading to the formation of tumours in the bone, liver, spleen, and adrenals/kidney [114–116], although lung metastases can be rate limiting with some models [105]. Alternative approaches include intracardiac injection, which disseminates cells *via* the arterial blood stream [117], or intra-caudal artery injection, which is technically simpler and allows entry into femoral artery and delivery cells to the bone marrow of hind limbs [118]. Experimental metastasis approaches have also been used to select cell populations with increased metastatic capacity by serial engraftment and isolation of metastases from specific organs [117]. Direct injection models have included a liver metastasis model where neuroblastoma cells are injected directly into the spleen of immunodeficient mice from where they can metastasize to the liver [119, 120], and bone metastasis model involving direct injection into of cells into the femur [121, 122].

3.5 PDX repositories, systematic pre-clinical testing initiatives, and personalized medicine

While individual neuroblastoma PDX models have been routinely utilized for pre-clinical assessment of individual anticancer agents [56, 93, 123–125], the greatest potential for realizing clinical benefit may come from the systematic application of PDX panels facilitated by large collections of diverse PDX models. The National Cancer Institute (NCI) Paediatric Preclinical Testing Consortium has conducted systematic testing of novel therapeutics in panels of paediatric cancer xenograft models, including neuroblastoma, for more than a decade [126] and has recently reported the development and genomic characterization of 35 high-risk neuroblastoma PDX models with a range of aberrations [85]. Similarly, the European Innovative Therapies for Children with Cancer (ITCC-P4) program aims to generate large panels of PDX models representing high-risk paediatric solid tumours to enable novel drug testing in partnership with industry. Xenograft repositories that bring together large collections of patient-derived xenograft models, such as the NCI Patient-Derived Models Repository, the Public Repository of Xenografts [127], The Children's Oncology Group (COG) Childhood Cancer Repository and the Childhood Solid Tumour Network (CSTN) established at St. Jude Children's Research Hospital [128] play important roles in access to models, as do PDX model development initiatives within personalized medicine clinical trials. Large collections of PDX models create opportunities for more thorough and representative pre-clinical evaluation of drug efficacy through more clinical trial like studies using single mouse designs [129] and have the potential to accelerate biomarker development [127]. Consistent and robust standards for PDX models and their associated clinical data have recently been proposed [130] and should allow standardization across PDX repositories, as well as consistency and reproducibility between pre-clinical studies that utilize them.

A developing area for neuroblastoma PDX models is integration into personalized oncology (Fig. 1) and PDX models utilized in this way are often referred to as “avatar” models. Xenografting can allow expansion of limited patient tumour material for additional profiling assays, including unbiased *ex vivo* drug sensitivity profiling [84]. Avatar PDX models also providing an *in vivo* platform for evidence-based validation and prioritization of therapeutic options identified by either by molecular methods or unbiased drug screening. Biobanking of PDX models may also allow similar PDX models to be used to support decision-making in the absence of a model for a given patient.

4 Conclusions

Animal models of high-risk neuroblastoma are central to better understanding tumorigenesis, tumour progression and

metastasis, validating tumour drivers and drug targets, conducting high-quality, informative assessment of new therapies and in supporting treatment decisions for individual patients. Complementary approaches to modelling high-risk neuroblastoma, including GEMM models of *MYCN*-amplified and *ALK*-mutant tumours, PDX models representing both the diversity of the human disease and individual patients, and models of disseminated disease each have important roles to play in these areas (Table 3). New directions for animal modelling of high-risk neuroblastoma will likely include GEMMs with complex recurrent aberrations developed using genome editing techniques, PDX models in humanized mice for assessment of immunotherapies and an increasingly important role for model repositories with consistent and rigorous data standards.

References

- Matthay, K. K., Maris, J. M., Schleiermacher, G., Nakagawara, A., Mackall, C. L., Diller, L., & Weiss, W. A. (2016). Neuroblastoma. *Nature Reviews Disease Primers*, 2, 16078.
- Marshall, G. M., Carter, D. R., Cheung, B. B., Liu, T., Mateos, M. K., Meyerowitz, J. G., & Weiss, W. A. (2014). The prenatal origins of cancer. *Nature Reviews Cancer*, 14(4), 277–289.
- Pugh, T. J., Morozova, O., Attiyeh, E. F., Asgharzadeh, S., Wei, J. S., Auclair, D., Carter, S. L., Cibulskis, K., Hanna, M., Kiezun, A., Kim, J., Lawrence, M. S., Lichtenstein, L., McKenna, A., Peadarallu, C. S., Ramos, A. H., Shefler, E., Sivachenko, A., Sougnez, C., Stewart, C., Ally, A., Birol, I., Chiu, R., Corbett, R. D., Hirst, M., Jackman, S. D., Kamoh, B., Khodabakhshi, A. H., Krzywinski, M., Lo, A., Moore, R. A., Mungall, K. L., Qian, J., Tam, A., Thiessen, N., Zhao, Y., Cole, K. A., Diamond, M., Diskin, S. J., Mosse, Y. P., Wood, A. C., Ji, L., Spoto, R., Badgett, T., London, W. B., Moyer, Y., Gastier-Foster, J. M., Smith, M. A., Guidry Auvil, J. M., Gerhard, D. S., Hogarty, M. D., Jones, S. J., Lander, E. S., Gabriel, S. B., Getz, G., Seeger, R. C., Khan, J., Marra, M. A., Meyerson, M., & Maris, J. M. (2013). The genetic landscape of high-risk neuroblastoma. *Nature Genetics*, 45(3), 279–284.
- Grobner, S. N., Worst, B. C., Weischenfeldt, J., Buchhalter, I., Kleinheinz, K., Rudneva, V. A., et al. (2018). The landscape of genomic alterations across childhood cancers. *Nature*, 555(7696), 321–327.
- Ma, X., Liu, Y., Liu, Y., Alexandrov, L. B., Edmonson, M. N., Gawad, C., Zhou, X., Li, Y., Rusch, M. C., Easton, J., Huether, R., Gonzalez-Pena, V., Wilkinson, M. R., Hermida, L. C., Davis, S., Sioson, E., Pounds, S., Cao, X., Ries, R. E., Wang, Z., Chen, X., Dong, L., Diskin, S. J., Smith, M. A., Guidry Auvil, J. M., Meltzer, P. S., Lau, C. C., Perlman, E. J., Maris, J. M., Meshinchi, S., Hunger, S. P., Gerhard, D. S., & Zhang, J. (2018). Pan-cancer genome and transcriptome analyses of 1,699 paediatric leukaemias and solid tumours. *Nature*, 555(7696), 371–376.
- Weiss, W., Aldape, K., Mohapatra, G., Feuerstein, B., & Bishop, J. (1997). Targeted expression of *MYCN* causes neuroblastoma in transgenic mice. *The EMBO Journal*, 16, 2985–2995.
- Heukamp, L. C., Thor, T., Schramm, A., De Preter, K., Kumps, C., De Wilde, B., et al. (2012). Targeted expression of mutated *ALK* induces neuroblastoma in transgenic mice. *Science Translational Medicine*, 4(141), 141ra191.
- Berry, T., Luther, W., Bhatnagar, N., Jamin, Y., Poon, E., Sanda, T., Pei, D., Sharma, B., Vetharoy, W. R., Hallsworth, A., Ahmad, Z., Barker, K., Moreau, L., Webber, H., Wang, W., Liu, Q., Perez-Atayde, A., Rodig, S., Cheung, N. K., Raynaud, F., Hallberg, B., Robinson, S. P., Gray, N. S., Pearson, A. D., Eccles, S. A., Chesler, L., & George, R. E. (2012). The *ALK*(F1174L) mutation potentiates the oncogenic activity of *MYCN* in neuroblastoma. *Cancer Cell*, 22(1), 117–130.
- Ueda, T., Nakata, Y., Yamasaki, N., Oda, H., Sentani, K., Kanai, A., Onishi, N., Ikeda, K., Sera, Y., Honda, Z. I., Tanaka, K., Sata, M., Ogawa, S., Yasui, W., Saya, H., Takita, J., & Honda, H. (2016). *ALK*(R1275Q) perturbs extracellular matrix, enhances cell invasion and leads to the development of neuroblastoma in cooperation with *MYCN*. *Oncogene*, 35(34), 4447–4458.
- Molenaar, J. J., Domingo-Fernandez, R., Ebus, M. E., Lindner, S., Koster, J., Drabek, K., et al. (2012). *LIN28B* induces neuroblastoma and enhances *MYCN* levels via *let-7* suppression. *Nature Genetics*, 44(11), 1199–1206.
- Hansford, L. M., Thomas, W. D., Keating, J. M., Burkhart, C. A., Peaston, A. E., Norris, M. D., Haber, M., Armati, P. J., Weiss, W. A., & Marshall, G. M. (2004). Mechanisms of embryonal tumor initiation: distinct roles for *MycN* expression and *MYCN* amplification. *Proceedings of the National Academy of Sciences of the United States of America*, 101(34), 12664–12669.
- Alam, G., Cui, H., Shi, H., Yang, L., Ding, J., Mao, L., Maltese, W. A., & Ding, H. F. (2009). *MYCN* promotes the expansion of *Phox2B*-positive neuronal progenitors to drive neuroblastoma development. *The American Journal of Pathology*, 175(2), 856–866.
- Beckwith, J. B., & Perrin, E. V. (1963). *In situ* neuroblastomas: a contribution to the natural history of neural crest tumors. *The American Journal of Pathology*, 43, 1089–1104.
- Rasmuson, A., Segerstrom, L., Nethander, M., Finnman, J., Elfman, L. H., Javanmardi, N., et al. (2012). Tumor development, growth characteristics and spectrum of genetic aberrations in the TH-*MYCN* mouse model of neuroblastoma. *PLoS One*, 7(12), e51297.
- Weiss, W. A., Godfrey, T., Francisco, C., & Bishop, J. M. (2000). Genome-wide screen for allelic imbalance in a mouse model for neuroblastoma. *Cancer Research*, 60(9), 2483–2487.
- Althoff, K., Beckers, A., Bell, E., Nortmeyer, M., Thor, T., Sprussel, A., et al. (2015). A Cre-conditional *MYCN*-driven neuroblastoma mouse model as an improved tool for preclinical studies. *Oncogene*, 34(26), 3357–3368.
- Hackett, C. S., Hodgson, J. G., Law, M. E., Fridlyand, J., Osoegawa, K., de Jong, P. J., Nowak, N. J., Pinkel, D., Albertson, D. G., Jain, A., Jenkins, R., Gray, J. W., & Weiss, W. A. (2003). Genome-wide array CGH analysis of murine neuroblastoma reveals distinct genomic aberrations which parallel those in human tumors. *Cancer Research*, 63(17), 5266–5273.
- Chesler, L., Goldenberg, D. D., Seales, I. T., Satchi-Fainaro, R., Grimmer, M., Collins, R., Struett, C., Nguyen, K. N., Kim, G., Tihan, T., Bao, Y., Brekken, R. A., Bergers, G., Folkman, J., & Weiss, W. A. (2007). Malignant progression and blockade of angiogenesis in a murine transgenic model of neuroblastoma. *Cancer Research*, 67(19), 9435–9442.
- Teitz, T., Stanke, J. J., Federico, S., Bradley, C. L., Brennan, R., Zhang, J., Johnson, M. D., Sedlacik, J., Inoue, M., Zhang, Z. M., Frase, S., Rehg, J. E., Hillenbrand, C. M., Finkelstein, D., Calabrese, C., Dyer, M. A., & Lahti, J. M. (2011). Preclinical models for neuroblastoma: establishing a baseline for treatment. *PLoS One*, 6(4), e19133.
- Jamin, Y., Tucker, E. R., Poon, E., Popov, S., Vaughan, L., Boulton, J. K., Webber, H., Hallsworth, A., Baker, L. C., Jones, C., Koh, D. M., Pearson, A. D., Chesler, L., & Robinson, S. P. (2013). Evaluation of clinically translatable MR imaging biomarkers of

- therapeutic response in the TH-MYCIN transgenic mouse model of neuroblastoma. *Radiology*, 266(1), 130–140.
21. Quarta, C., Cantelli, E., Nanni, C., Ambrosini, V., D'Ambrosio, D., Di Leo, K., et al. (2013). Molecular imaging of neuroblastoma progression in TH-MYCIN transgenic mice. *Molecular Imaging and Biology*, 15(2), 194–202.
 22. Accorsi, R., Morowitz, M. J., Charron, M., & Maris, J. M. (2003). Pinhole imaging of 131I-metaiodobenzylguanidine (131I-MIBG) in an animal model of neuroblastoma. *Pediatric Radiology*, 33(10), 688–692.
 23. Chesler, L., Goldenberg, D. D., Collins, R., Grimmer, M., Kim, G. E., Tihan, T., Nguyen, K., Yakovenko, S., Matthay, K. K., & Weiss, W. A. (2008). Chemotherapy-induced apoptosis in a transgenic model of neuroblastoma proceeds through p53 induction. *Neoplasia*, 10(11), 1268–1274.
 24. Janoueix-Lerosey, I., Lequin, D., Brugieres, L., Ribeiro, A., de Pontual, L., Combaret, V., et al. (2008). Somatic and germline activating mutations of the ALK kinase receptor in neuroblastoma. *Nature*, 455(7215), 967–970.
 25. Mosse, Y. P., Laudenslager, M., Longo, L., Cole, K. A., Wood, A., Attiyeh, E. F., et al. (2008). Identification of ALK as a major familial neuroblastoma predisposition gene. *Nature*, 455(7215), 930–935.
 26. Bresler, S. C., Weiser, D. A., Huwe, P. J., Park, J. H., Krytska, K., Ryles, H., Laudenslager, M., Rappaport, E. F., Wood, A. C., McGrady, P., Hogarty, M. D., London, W. B., Radhakrishnan, R., Lemmon, M. A., & Mossé, Y. P. (2014). ALK mutations confer differential oncogenic activation and sensitivity to ALK inhibition therapy in neuroblastoma. *Cancer Cell*, 26(5), 682–694.
 27. De Wilde, B., Beckers, A., Lindner, S., Kristina, A., De Preter, K., Depuydt, P., et al. (2018). The mutational landscape of MYCN, Lin28b and ALK(F1174L) driven murine neuroblastoma mimics human disease. *Oncotarget*, 9(9), 8334–8349.
 28. Viswanathan, S. R., Daley, G. Q., & Gregory, R. I. (2008). Selective blockade of microRNA processing by Lin28. *Science*, 320(5872), 97–100.
 29. Buechner, J., Tomte, E., Haug, B. H., Henriksen, J. R., Lokke, C., Flaegstad, T., et al. (2011). Tumour-suppressor microRNAs let-7 and mir-101 target the proto-oncogene MYCN and inhibit cell proliferation in MYCN-amplified neuroblastoma. *British Journal of Cancer*, 105(2), 296–303.
 30. Diskin, S. J., Capasso, M., Schnepf, R. W., Cole, K. A., Attiyeh, E. F., Hou, C., Diamond, M., Carpenter, E. L., Winter, C., Lee, H., Jagannathan, J., Latorre, V., Iolascon, A., Hakonarson, H., Devoto, M., & Maris, J. M. (2012). Common variation at 6q16 within HACE1 and LIN28B influences susceptibility to neuroblastoma. *Nature Genetics*, 44(10), 1126–1130.
 31. Yogeve, O., Barker, K., Sikka, A., Almeida, G. S., Hallsworth, A., Smith, L. M., Jamin, Y., Ruddell, R., Koers, A., Webber, H. T., Raynaud, F. I., Popov, S., Jones, C., Petrie, K., Robinson, S. P., Keun, H. C., & Chesler, L. (2016). p53 loss in MYC-driven neuroblastoma leads to metabolic adaptations supporting radioresistance. *Cancer Research*, 76(10), 3025–3035.
 32. Chmielecki, J., Bailey, M., He, J., Elvin, J., Vergilio, J. A., Ramkissoon, S., Suh, J., Frampton, G. M., Sun, J. X., Morley, S., Spritz, D., Ali, S., Gay, L., Erlich, R. L., Ross, J. S., Buxhaku, J., Davies, H., Faso, V., Germain, A., Glanville, B., Miller, V. A., Stephens, P. J., Janeway, K. A., Maris, J. M., Meshinchi, S., Pugh, T. J., Shern, J. F., & Lipson, D. (2017). Genomic profiling of a large set of diverse pediatric cancers identifies known and novel mutations across tumor spectra. *Cancer Research*, 77(2), 509–519.
 33. Carr-Wilkinson, J., O'Toole, K., Wood, K. M., Challen, C. C., Baker, A. G., Board, J. R., Evans, L., Cole, M., Cheung, N. K., Boos, J., Köhler, G., Leuschner, I., Pearson, A. D., Lunec, J., & Tweddle, D. A. (2010). High frequency of p53/MDM2/p14ARF pathway abnormalities in relapsed Neuroblastoma. *Clinical Cancer Research*, 16(4), 1108–1118.
 34. Padovan-Merhar, O. M., Raman, P., Ostrovskaya, I., Kalletta, K., Rubnitz, K. R., Sanford, E. M., Ali, S. M., Miller, V. A., Mossé, Y. P., Granger, M. P., Weiss, B., Maris, J. M., & Modak, S. (2016). Enrichment of targetable mutations in the relapsed neuroblastoma genome. *PLoS Genetics*, 12(12), e1006501.
 35. Eleveld, T. F., Oldridge, D. A., Bernard, V., Koster, J., Daage, L. C., Diskin, S. J., et al. (2015). Relapsed neuroblastomas show frequent RAS-MAPK pathway mutations. *Nature Genetics*, 47(8), 864–871.
 36. Nakamura, T., Iwamura, Y., Kaneko, M., Nakagawa, K., Kawai, K., Mitamura, K., Futagawa, T., & Hayashi, H. (1991). Deletions and rearrangements of the retinoblastoma gene in hepatocellular carcinoma, insulinoma and some neurogenic tumors as found in a study of 121 tumors. *Japanese Journal of Clinical Oncology*, 21(5), 325–329.
 37. Chayka, O., Corvetta, D., Dews, M., Caccamo, A. E., Piotrowska, I., Santilli, G., Gibson, S., Sebire, N. J., Himoudi, N., Hogarty, M. D., Anderson, J., Bettuzzi, S., Thomas-Tikhonenko, A., & Sala, A. (2009). Clusterin, a haploinsufficient tumor suppressor gene in neuroblastomas. *Journal of the National Cancer Institute*, 101(9), 663–677.
 38. Teitz, T., Inoue, M., Valentine, M. B., Zhu, K., Reh, J. E., Zhao, W., Finkelstein, D., Wang, Y. D., Johnson, M. D., Calabrese, C., Rubinstein, M., Hakem, R., Weiss, W. A., & Lahti, J. M. (2013). Th-MYCIN mice with caspase-8 deficiency develop advanced neuroblastoma with bone marrow metastasis. *Cancer Research*, 73(13), 4086–4097.
 39. Grau, E., Martinez, F., Orellana, C., Canete, A., Yanez, Y., Oltra, S., et al. (2011). Hypermethylation of apoptotic genes as independent prognostic factor in neuroblastoma disease. *Molecular Carcinogenesis*, 50(3), 153–162.
 40. Teitz, T., Wei, T., Valentine, M. B., Vanin, E. F., Grenet, J., Valentine, V. A., Behm, F. G., Look, A. T., Lahti, J. M., & Kidd, V. J. (2000). Caspase 8 is deleted or silenced preferentially in childhood neuroblastomas with amplification of MYCN. *Nature Medicine*, 6(5), 529–535.
 41. Stupack, D. G., Teitz, T., Potter, M. D., Mikolon, D., Houghton, P. J., Kidd, V. J., Lahti, J. M., & Cheresch, D. A. (2006). Potentiation of neuroblastoma metastasis by loss of caspase-8. *Nature*, 439(7072), 95–99.
 42. Schleiermacher, G., Javanmardi, N., Bernard, V., Leroy, Q., Cappo, J., Rio Frio, T., Pierron, G., Lapouble, E., Combaret, V., Speleman, F., de Wilde, B., Djos, A., Ora, I., Hedborg, F., Träger, C., Holmqvist, B. M., Abrahamsson, J., Peuchmaur, M., Michon, J., Janoueix-Lerosey, I., Kogner, P., Delattre, O., & Martinsson, T. (2014). Emergence of new ALK mutations at relapse of neuroblastoma. *Journal of Clinical Oncology*, 32(25), 2727–2734.
 43. Suenaga, Y., Islam, S. M., Alagu, J., Kaneko, Y., Kato, M., Tanaka, Y., Kawana, H., Hossain, S., Matsumoto, D., Yamamoto, M., Shoji, W., Itami, M., Shibata, T., Nakamura, Y., Ohira, M., Haraguchi, S., Takatori, A., & Nakagawara, A. (2014). NCYM, a Cis-antisense gene of MYCN, encodes a de novo evolved protein that inhibits GSK3beta resulting in the stabilization of MYCN in human neuroblastomas. *PLoS Genetics*, 10(1), e1003996.
 44. Chen, Z., Lin, Y., Barbieri, E., Burlingame, S., Hicks, J., Ludwig, A., & Shohet, J. M. (2009). Mdm2 deficiency suppresses MYCN-Driven neuroblastoma tumorigenesis in vivo. *Neoplasia*, 11(8), 753–762.
 45. Kishida, S., Mu, P., Miyakawa, S., Fujiwara, M., Abe, T., Sakamoto, K., Onishi, A., Nakamura, Y., & Kadomatsu, K. (2013). Midkine promotes neuroblastoma through Notch2 signaling. *Cancer Research*, 73(4), 1318–1327.

46. Ikematsu, S., Nakagawara, A., Nakamura, Y., Ohira, M., Shinjo, M., Kishida, S., & Kadomatsu, K. (2008). Plasma midkine level is a prognostic factor for human neuroblastoma. *Cancer Science*, *99*(10), 2070–2074.
47. Dorstyn, L., Puccini, J., Nikolic, A., Shalini, S., Wilson, C. H., Norris, M. D., et al. (2014). An unexpected role for caspase-2 in neuroblastoma. *Cell Death & Disease*, *5*, e1383.
48. Burkhardt, C. A., Watt, F., Murray, J., Pajic, M., Prokvolit, A., Xue, C., Flemming, C., Smith, J., Purnal, A., Isachenko, N., Komarov, P. G., Gurova, K. V., Sartorelli, A. C., Marshall, G. M., Norris, M. D., Gudkov, A. V., & Haber, M. (2009). Small-molecule multi-drug resistance-associated protein 1 inhibitor reversan increases the therapeutic index of chemotherapy in mouse models of neuroblastoma. *Cancer Research*, *69*(16), 6573–6580.
49. Henderson, M. J., Haber, M., Porro, A., Munoz, M. A., Iraci, N., Xue, C., Murray, J., Flemming, C. L., Smith, J., Fletcher, J. I., Gherardi, S., Kwek, C. K., Russell, A. J., Valli, E., London, W. B., Buxton, A. B., Ashton, L. J., Sartorelli, A. C., Cohn, S. L., Schwab, M., Marshall, G. M., Perini, G., & Norris, M. D. (2011). ABCG2 multidrug transporters in childhood neuroblastoma: clinical and biological effects independent of cytotoxic drug efflux. *Journal of the National Cancer Institute*, *103*(16), 1236–1251.
50. Haber, M., Smith, J., Bordow, S. B., Flemming, C., Cohn, S. L., London, W. B., Marshall, G. M., & Norris, M. D. (2006). Association of high-level MRP1 expression with poor clinical outcome in a large prospective study of primary neuroblastoma. *Journal of Clinical Oncology*, *24*(10), 1546–1553.
51. Murray, J., Valli, E., Yu, D. M. T., Truong, A. M., Gifford, A. J., Eden, G. L., Gamble, L. D., Hanssen, K. M., Flemming, C. L., Tan, A., Tivnan, A., Allan, S., Saletta, F., Cheung, L., Ruhle, M., Schuetz, J. D., Henderson, M. J., Byrne, J. A., Norris, M. D., Haber, M., & Fletcher, J. I. (2017). Suppression of the ATP-binding cassette transporter ABCG4 impairs neuroblastoma tumour growth and sensitises to irinotecan in vivo. *European Journal of Cancer*, *83*, 132–141.
52. Norris, M. D., Smith, J., Tanabe, K., Tobin, P., Flemming, C., Scheffer, G. L., Wielinga, P., Cohn, S. L., London, W. B., Marshall, G. M., Allen, J. D., & Haber, M. (2005). Expression of multidrug transporter MRP4/ABCC4 is a marker of poor prognosis in neuroblastoma and confers resistance to irinotecan in vitro. *Molecular Cancer Therapeutics*, *4*(4), 547–553.
53. Hogarty, M. D., Norris, M. D., Davis, K., Liu, X., Evageliou, N. F., Hayes, C. S., Pawel, B., Guo, R., Zhao, H., Sekyere, E., Keating, J., Thomas, W., Cheng, N. C., Murray, J., Smith, J., Sutton, R., Venn, N., London, W. B., Buxton, A., Gilmour, S. K., Marshall, G. M., & Haber, M. (2008). ODC1 is a critical determinant of MYCN oncogenesis and a therapeutic target in neuroblastoma. *Cancer Research*, *68*(23), 9735–9745.
54. Carter, D. R., Murray, J., Cheung, B. B., Gamble, L., Koach, J., Tsang, J., et al. (2015). Therapeutic targeting of the MYC signal by inhibition of histone chaperone FACT in neuroblastoma. *Science Translational Medicine*, *7*(312), 312ra176.
55. Evageliou, N. F., Haber, M., Vu, A., Laetsch, T. W., Murray, J., Gamble, L. D., Cheng, N. C., Liu, K., Reese, M., Corrigan, K. A., Ziegler, D. S., Webber, H., Hayes, C. S., Pawel, B., Marshall, G. M., Zhao, H., Gilmour, S. K., Norris, M. D., & Hogarty, M. D. (2016). Polyamine antagonist therapies inhibit neuroblastoma initiation and progression. *Clinical Cancer Research*, *22*(17), 4391–4404.
56. Gamble, L. D., Purgato, S., Murray, J., Xiao, L., Yu, D. M. T., Hanssen, K. M., et al. (2019). Inhibition of polyamine synthesis and uptake reduces tumor progression and prolongs survival in mouse models of neuroblastoma. *Science Translational Medicine*, *11*(477).
57. Yogev, O., Almeida, G. S., Barker, K. T., George, S. L., Kwok, C., Campbell, J., Zarowiecki, M., Klefogiannis, D., Smith, L. M., Hallsworth, A., Berry, P., Möcklinghoff, T., Webber, H. T., Danielson, L. S., Buttery, B., Calton, E. A., da Costa, B. M., Poon, E., Jamin, Y., Lise, S., Veal, G. J., Sebire, N., Robinson, S. P., Anderson, J., & Chesler, L. (2019). In vivo modeling of chemoresistant neuroblastoma provides new insights into chemorefractory disease and metastasis. *Cancer Research*, *79*(20), 5382–5393.
58. Liu, T., Tee, A. E., Porro, A., Smith, S. A., Dwarte, T., Liu, P. Y., Iraci, N., Sekyere, E., Haber, M., Norris, M. D., Diolaiti, D., Della Valle, G., Perini, G., & Marshall, G. M. (2007). Activation of tissue transglutaminase transcription by histone deacetylase inhibition as a therapeutic approach for Myc oncogenesis. *Proceedings of the National Academy of Sciences of the United States of America*, *104*(47), 18682–18687.
59. Waldeck, K., Cullinane, C., Ardley, K., Shortt, J., Martin, B., Tohill, R. W., Li, J., Johnstone, R. W., McArthur, G., Hicks, R. J., & Wood, P. J. (2016). Long term, continuous exposure to panobinostat induces terminal differentiation and long term survival in the TH-MYCN neuroblastoma mouse model. *International Journal of Cancer*, *139*(1), 194–204.
60. Faisal, A., Vaughan, L., Bavetsias, V., Sun, C., Atrash, B., Avery, S., Jamin, Y., Robinson, S. P., Workman, P., Blagg, J., Raynaud, F. I., Eccles, S. A., Chesler, L., & Linardopoulos, S. (2011). The aurora kinase inhibitor CCT137690 downregulates MYCN and sensitizes MYCN-amplified neuroblastoma in vivo. *Molecular Cancer Therapeutics*, *10*(11), 2115–2123.
61. Brockmann, M., Poon, E., Berry, T., Carstensen, A., Deubzer, H. E., Rycak, L., Jamin, Y., Thway, K., Robinson, S. P., Roels, F., Witt, O., Fischer, M., Chesler, L., & Eilers, M. (2013). Small molecule inhibitors of aurora-a induce proteasomal degradation of N-myc in childhood neuroblastoma. *Cancer Cell*, *24*(1), 75–89.
62. Puissant, A., Frumm, S. M., Alexe, G., Bassil, C. F., Qi, J., Chanthery, Y. H., Nekritz, E. A., Zeid, R., Gustafson, W. C., Greninger, P., Garnett, M. J., McDermott, U., Benes, C. H., Kung, A. L., Weiss, W. A., Bradner, J. E., & Stegmaier, K. (2013). Targeting MYCN in neuroblastoma by BET bromodomain inhibition. *Cancer Discovery*, *3*(3), 308–323.
63. Dolman, M. E., Poon, E., Ebus, M. E., den Hartog, I. J., van Noesel, C. J., Jamin, Y., et al. (2015). Cyclin-dependent kinase inhibitor AT7519 as a potential drug for MYCN-dependent neuroblastoma. *Clinical Cancer Research*, *21*(22), 5100–5109.
64. Koach, J., Holien, J. K., Massudi, H., Carter, D. R., Ciampa, O. C., Herath, M., Lim, T., Seneviratne, J. A., Milazzo, G., Murray, J. E., McCarroll, J., Liu, B., Mayoh, C., Keenan, B., Stevenson, B. W., Gorman, M. A., Bell, J. L., Doughly, L., Hüttelmaier, S., Oberthuer, A., Fischer, M., Gifford, A. J., Liu, T., Zhang, X., Zhu, S., Gustafson, W. C., Haber, M., Norris, M. D., Fletcher, J. I., Perini, G., Parker, M. W., Cheung, B. B., & Marshall, G. M. (2019). Drugging MYCN oncogenic signaling through the MYCN-PA2G4 binding interface. *Cancer Research*, *79*(21), 5652–5667.
65. Chesler, L., & Weiss, W. A. (2011). Genetically engineered murine models—contribution to our understanding of the genetics, molecular pathology and therapeutic targeting of neuroblastoma. *Seminars in Cancer Biology*, *21*(4), 245–255.
66. Kiyonari, S., & Kadomatsu, K. (2015). Neuroblastoma models for insights into tumorigenesis and new therapies. *Expert Opinion on Drug Discovery*, *10*(1), 53–62.
67. Galluzzi, L., Senovilla, L., Zitvogel, L., & Kroemer, G. (2012). The secret ally: immunostimulation by anticancer drugs. *Nature Reviews. Drug Discovery*, *11*(3), 215–233.
68. Kroesen, M., Nierkens, S., Ansems, M., Wassink, M., Orentas, R. J., Boon, L., den Brok, M., Hoogerbrugge, P. M., & Adema, G. J. (2014). A transplantable TH-MYCN transgenic tumor model in C57Bl/6 mice for preclinical immunological studies in neuroblastoma. *International Journal of Cancer*, *134*(6), 1335–1345.

69. Kroesen, M., Bull, C., Gielen, P. R., Brok, I. C., Armandari, I., Wassink, M., et al. (2016). Anti-GD2 mAb and Vorinostat synergize in the treatment of neuroblastoma. *Oncoimmunology*, 5(6), e1164919.
70. Mao, Y., Eissler, N., Blanc, K. L., Johnsen, J. I., Kogner, P., & Kiessling, R. (2016). Targeting suppressive myeloid cells potentiates checkpoint inhibitors to control spontaneous neuroblastoma. *Clinical Cancer Research*, 22(15), 3849–3859.
71. Hidalgo, M., Amant, F., Biankin, A. V., Budinska, E., Byrne, A. T., Caldas, C., et al. (2014). Patient-derived xenograft models: an emerging platform for translational cancer research. *Cancer Discovery*, 4(9), 998–1013.
72. Hidalgo, M., Bruckheimer, E., Rajeshkumar, N. V., Garrido-Laguna, I., De Oliveira, E., Rubio-Viqueira, B., et al. (2011). A pilot clinical study of treatment guided by personalized tumorgrafts in patients with advanced cancer. *Molecular Cancer Therapeutics*, 10(8), 1311–1316.
73. Blattmann, C., Thiemann, M., Stenzinger, A., Roth, E. K., Dittmar, A., Witt, H., et al. (2015). Establishment of a patient-derived orthotopic osteosarcoma mouse model. *Journal of Translational Medicine*, 13, 136.
74. Kim, M. P., Evans, D. B., Wang, H., Abbruzzese, J. L., Fleming, J. B., & Gallick, G. E. (2009). Generation of orthotopic and heterotopic human pancreatic cancer xenografts in immunodeficient mice. *Nature Protocols*, 4(11), 1670–1680.
75. Monsma, D. J., Monks, N. R., Cherba, D. M., Dylewski, D., Eugster, E., Jahn, H., et al. (2012). Genomic characterization of explant tumorgraft models derived from fresh patient tumor tissue. *Journal of Translational Medicine*, 10, 125.
76. Daniel, V. C., Marchionni, L., Hierman, J. S., Rhodes, J. T., Devereux, W. L., Rudin, C. M., Yung, R., Parmigiani, G., Dorsch, M., Peacock, C. D., & Watkins, D. N. (2009). A primary xenograft model of small-cell lung cancer reveals irreversible changes in gene expression imposed by culture in vitro. *Cancer Research*, 69(8), 3364–3373.
77. Tentler, J. J., Tan, A. C., Weekes, C. D., Jimeno, A., Leong, S., Pitts, T. M., Arcaroli, J. J., Messersmith, W. A., & Eckhardt, S. G. (2012). Patient-derived tumour xenografts as models for oncology drug development. *Nature Reviews. Clinical Oncology*, 9(6), 338–350.
78. Tsuchida, Y., Yokomori, K., Iwanaka, T., & Saito, S. (1984). Nude mouse xenograft study for treatment of neuroblastoma: effects of chemotherapeutic agents and surgery on tumor growth and cell kinetics. *Journal of Pediatric Surgery*, 19(1), 72–76.
79. Tsuchida, Y., Kanda, N., Shimatake, H., Kaneko, Y., & Notomi, T. (1988). Clinical significance of gene amplification studied in human neuroblastoma xenografts: relationship with tumor growth rate, chemotherapeutic sensitivities and levels of neuron-specific enolase. *Experimental Cell Biology*, 56(5), 277–284.
80. George, B. A., Yanik, G., Wells, R. J., Martin, L. W., Soukup, S., Ballard, E. T., Gartside, P. S., & Lampkin, B. C. (1993). Growth patterns of human neuroblastoma xenografts and their relationship to treatment outcome. *Cancer*, 72(11), 3331–3339.
81. Johnson, J. I., Decker, S., Zaharevitz, D., Rubinstein, L. V., Venditti, J. M., Schepartz, S., et al. (2001). Relationships between drug activity in NCI preclinical in vitro and in vivo models and early clinical trials. *British Journal of Cancer*, 84(10), 1424–1431.
82. Zarzosa, P., Navarro, N., Giralt, I., Molist, C., Almazan-Moga, A., Vidal, I., et al. (2017). Patient-derived xenografts for childhood solid tumors: a valuable tool to test new drugs and personalize treatments. *Clinical & Translational Oncology*, 19(1), 44–50.
83. Stewart, E., Federico, S. M., Chen, X., Shelat, A. A., Bradley, C., Gordon, B., Karlstrom, A., Twarog, N. R., Clay, M. R., Bahrami, A., Freeman 3rd, B. B., Xu, B., Zhou, X., Wu, J., Honnell, V., Ocarz, M., Blankenship, K., Dapper, J., Mardis, E. R., Wilson, R. K., Downing, J., Zhang, J., Easton, J., Pappo, A., & Dyer, M. A. (2017). Orthotopic patient-derived xenografts of paediatric solid tumours. *Nature*, 549(7670), 96–100.
84. Kamili, A., Gifford, A. J., Li, N., Mayoh, C., Chow, S., Faires, T. W., et al. (2020). Accelerating development of high-risk neuroblastoma patient-derived xenograft models for pre-clinical testing and personalised therapy. *British Journal of Cancer*. <https://doi.org/10.1038/s41416-019-0682-4>.
85. Rokita, J. L., Rathi, K. S., Cardenas, M. F., Upton, K. A., Jayaseelan, J., Cross, K. L., et al. (2019). Genomic profiling of childhood tumor patient-derived xenograft models to enable rational clinical trial design. *Cell Reports*, 29(6), 1675–1689.e1679.
86. Ito, R., Katano, I., Kawai, K., Hirata, H., Ogura, T., Kamisako, T., Eto, T., & Ito, M. (2009). Highly sensitive model for xenogenic GVHD using severe immunodeficient NOG mice. *Transplantation*, 87(11), 1654–1658.
87. Bondarenko, G., Ugoikov, A., Rohan, S., Kulesza, P., Dubrovskiy, O., Gursel, D., Mathews, J., O'Halloran, T. V., Wei, J. J., & Mazar, A. P. (2015). Patient-derived tumor xenografts are susceptible to formation of human lymphocytic tumors. *Neoplasia*, 17(9), 735–741.
88. Zhang, L., Liu, Y., Wang, X., Tang, Z., Li, S., Hu, Y., et al. (2015). The extent of inflammatory infiltration in primary cancer tissues is associated with lymphomagenesis in immunodeficient mice. *Scientific Reports*, 5, 9447.
89. Wetterauer, C., Vlajnic, T., Schuler, J., Gsponer, J. R., Thalmann, G. N., Cecchini, M., et al. (2015). Early development of human lymphomas in a prostate cancer xenograft program using triple knock-out immunocompromised mice. *Prostate*, 75(6), 585–592.
90. Braekeveldt, N., Wigerup, C., Gisselsson, D., Mohlin, S., Merselius, M., Beckman, S., Jonson, T., Börjesson, A., Backman, T., Tadeo, I., Berbegall, A. P., Ora, I., Navarro, S., Noguera, R., Pählman, S., & Bexell, D. (2015). Neuroblastoma patient-derived orthotopic xenografts retain metastatic patterns and geno- and phenotypes of patient tumours. *International Journal of Cancer*, 136(5), E252–E261.
91. Read, M., Liu, D., Duong, C. P., Cullinane, C., Murray, W. K., Fennell, C. M., Shortt, J., Westerman, D., Burton, P., Clemons, N. J., & Phillips, W. A. (2016). Intramuscular transplantation improves engraftment rates for esophageal patient-derived tumor xenografts. *Annals of Surgical Oncology*, 23(1), 305–311.
92. Khanna, C., Jaboin, J. J., Drakos, E., Tsokos, M., & Thiele, C. J. (2002). Biologically relevant orthotopic neuroblastoma xenograft models: primary adrenal tumor growth and spontaneous distant metastasis. *In Vivo*, 16(2), 77–85.
93. Braekeveldt, N., & Bexell, D. (2018). Patient-derived xenografts as preclinical neuroblastoma models. *Cell and Tissue Research*, 372(2), 233–243.
94. Talmadge, J. E., Singh, R. K., Fidler, I. J., & Raz, A. (2007). Murine models to evaluate novel and conventional therapeutic strategies for cancer. *The American Journal of Pathology*, 170(3), 793–804.
95. Braekeveldt, N., Wigerup, C., Tadeo, I., Beckman, S., Sanden, C., Jonsson, J., et al. (2016). Neuroblastoma patient-derived orthotopic xenografts reflect the microenvironmental hallmarks of aggressive patient tumours. *Cancer Letters*, 375(2), 384–389.
96. Singh, Z. (2016). Applications and toxicity of graphene family nanomaterials and their composites. *Nanotechnology, Science and Applications*, 9, 15–28.
97. de la Fuente, A., Alonso-Alconada, L., Costa, C., Cueva, J., Garcia-Caballero, T., Lopez-Lopez, R., et al. (2015). M-trap: exosome-based capture of tumor cells as a new technology in peritoneal metastasis. *Journal of the National Cancer Institute*, 107(9).
98. Dong, Z., Imai, A., Krishnamurthy, S., Zhang, Z., Zeitlin, B. D., & Nor, J. E. (2013). Xenograft tumors vascularized with murine blood vessels may overestimate the effect of anti-tumor drugs: a pilot study. *PLoS One*, 8(12), e84236.

99. Rubio-Viqueira, B., & Hidalgo, M. (2009). Direct in vivo xenograft tumor model for predicting chemotherapeutic drug response in cancer patients. *Clinical Pharmacology and Therapeutics*, 85(2), 217–221.
100. Stewart, E., Shelat, A., Bradley, C., Chen, X., Federico, S., Thiagarajan, S., Shirinifard, A., Bahrami, A., Pappo, A., Qu, C., Finkelstein, D., Sablauer, A., & Dyer, M. A. (2015). Development and characterization of a human orthotopic neuroblastoma xenograft. *Developmental Biology*, 407(2), 344–355.
101. Fuchs, D., Christofferson, R., Stridsberg, M., Lindhagen, E., & Azarbayjani, F. (2009). Regression of orthotopic neuroblastoma in mice by targeting the endothelial and tumor cell compartments. *Journal of Translational Medicine*, 7, 16.
102. Svensson, A., Backman, U., Jonsson, E., Larsson, R., & Christofferson, R. (2002). CHS 828 inhibits neuroblastoma growth in mice alone and in combination with antiangiogenic drugs. *Pediatric Research*, 51(5), 607–611.
103. Henriksson, K. C., Almgren, M. A., Thurlow, R., Varki, N. M., & Chang, C. L. (2004). A fluorescent orthotopic mouse model for reliable measurement and genetic modulation of human neuroblastoma metastasis. *Clinical & Experimental Metastasis*, 21(6), 563–570.
104. Dickson, P. V., Hamner, B., Ng, C. Y., Hall, M. M., Zhou, J., Hargrove, P. W., McCarville, M., & Davidoff, A. M. (2007). In vivo bioluminescence imaging for early detection and monitoring of disease progression in a murine model of neuroblastoma. *Journal of Pediatric Surgery*, 42(7), 1172–1179.
105. Daudigeos-Dubus, E., LE, D. L., Rouffiac, V., Bawa, O., Leguermey, I., Opolon, P., et al. (2014). Establishment and characterization of new orthotopic and metastatic neuroblastoma models. *In Vivo*, 28(4), 425–434.
106. Abbasi, M. R., Rifatbegovic, F., Brunner, C., Mann, G., Ziegler, A., Potschger, U., et al. (2017). Impact of disseminated neuroblastoma cells on the identification of the relapse-seeding clone. *Clinical Cancer Research*, 23(15), 4224–4232.
107. DuBois, S. G., Kalika, Y., Lukens, J. N., Brodeur, G. M., Seeger, R. C., Atkinson, J. B., et al. (1999). Metastatic sites in stage IV and IVS neuroblastoma correlate with age, tumor biology, and survival. *Journal of Pediatric Hematology/Oncology*, 21(3), 181–189.
108. Kramer, K., Kushner, B., Heller, G., & Cheung, N. K. (2001). Neuroblastoma metastatic to the central nervous system. The memorial Sloan-Kettering cancer center experience and a literature review. *Cancer*, 91(8), 1510–1519.
109. Morgenstern, D. A., London, W. B., Stephens, D., Volchenboun, S. L., Simon, T., Nakagawara, A., Shimada, H., Schleiermacher, G., Matthay, K. K., Cohn, S. L., Pearson, A. D., & Irwin, M. S. (2016). Prognostic significance of pattern and burden of metastatic disease in patients with stage 4 neuroblastoma: a study from the International Neuroblastoma Risk Group database. *European Journal of Cancer*, 65, 1–10.
110. Almgren, M. A., Henriksson, K. C., Fujimoto, J., & Chang, C. L. (2004). Nucleoside diphosphate kinase A/nm23-H1 promotes metastasis of NB69-derived human neuroblastoma. *Molecular Cancer Research*, 2(7), 387–394.
111. Hanna, C., Kwok, L., Finlay-Schultz, J., Sartorius, C. A., & Citty, D. M. (2016). Labeling of breast Cancer patient-derived Xenografts with traceable reporters for tumor growth and metastasis studies. *Journal of Visualized Experiments*, 117.
112. Jackson, J. R., Kim, Y., Seeger, R. C., & Kim, E. S. (2016). A novel minimal residual disease model of neuroblastoma in mice. *Journal of Pediatric Surgery*, 51(6), 991–994.
113. Barry, W. E., Jackson, J. R., Asuelime, G. E., Wu, H. W., Sun, J., Wan, Z., Malvar, J., Sheard, M. A., Wang, L., Seeger, R. C., & Kim, E. S. (2019). Activated natural killer cells in combination with anti-GD2 antibody dinutuximab improve survival of mice after surgical resection of primary neuroblastoma. *Clinical Cancer Research*, 25(1), 325–333.
114. Bogenmann, E. (1996). A metastatic neuroblastoma model in SCID mice. *International Journal of Cancer*, 67(3), 379–385.
115. Zhang, L., Smith, K. M., Chong, A. L., Stempak, D., Yeger, H., Marrano, P., Thorner, P. S., Irwin, M. S., Kaplan, D. R., & Baruchel, S. (2009). In vivo antitumor and antimetastatic activity of sunitinib in preclinical neuroblastoma mouse model. *Neoplasia*, 11(5), 426–435.
116. Muhlethaler-Mottet, A., Liberman, J., Ascencio, K., Flahaut, M., Balmas Bourlout, K., Yan, P., et al. (2015). The CXCR4/CXCR7/CXCL12 axis is involved in a secondary but complex control of neuroblastoma metastatic cell homing. *PLoS One*, 10(5), e0125616.
117. Seong, B. K., Fathers, K. E., Hallett, R., Yung, C. K., Stein, L. D., Mouaaz, S., Kee, L., Hawkins, C. E., Irwin, M. S., & Kaplan, D. R. (2017). A metastatic mouse model identifies genes that regulate neuroblastoma metastasis. *Cancer Research*, 77(3), 696–706.
118. Kuchimaru, T., Kataoka, N., Nakagawa, K., Isozaki, T., Miyabara, H., Minegishi, M., Kadonosono, T., & Kizaka-Kondoh, S. (2018). A reliable murine model of bone metastasis by injecting cancer cells through caudal arteries. *Nature Communications*, 9(1), 2981.
119. Lee, S., Qiao, J., Paul, P., O'Connor, K. L., Evers, M. B., & Chung, D. H. (2012). FAK is a critical regulator of neuroblastoma liver metastasis. *Oncotarget*, 3(12), 1576–1587.
120. Qiao, J., Kang, J., Ishola, T. A., Rychahou, P. G., Evers, B. M., & Chung, D. H. (2008). Gastrin-releasing peptide receptor silencing suppresses the tumorigenesis and metastatic potential of neuroblastoma. *Proceedings of the National Academy of Sciences of the United States of America*, 105(35), 12891–12896.
121. Sahara, Y., Shimada, H., Scadeng, M., Pollack, H., Yamada, S., Ye, W., Reynolds, C. P., & DeClerck, Y. (2003). Lytic bone lesions in human neuroblastoma xenograft involve osteoclast recruitment and are inhibited by bisphosphonate. *Cancer Research*, 63(12), 3026–3031.
122. Zhao, H., Cai, W., Li, S., Da, Z., Sun, H., Ma, L., et al. (2012). Establishment and characterization of xenograft models of human neuroblastoma bone metastasis. *Child's Nervous System*, 28(12), 2047–2054.
123. Mohlin, S., Hamidian, A., von Stedingk, K., Bridges, E., Wigerup, C., Bexell, D., & Pahlman, S. (2015). PI3K-mTORC2 but not PI3K-mTORC1 regulates transcription of HIF2A/EPAS1 and vascularization in neuroblastoma. *Cancer Research*, 75(21), 4617–4628.
124. Infarinato, N. R., Park, J. H., Krytska, K., Ryles, H. T., Sano, R., Szigety, K. M., Li, Y., Zou, H. Y., Lee, N. V., Smeal, T., Lemmon, M. A., & Mossé, Y. P. (2016). The ALK/ROS1 inhibitor PF-06463922 overcomes primary resistance to crizotinib in ALK-driven Neuroblastoma. *Cancer Discovery*, 6(1), 96–107.
125. Krytska, K., Ryles, H. T., Sano, R., Raman, P., Infarinato, N. R., Hansel, T. D., Makena, M. R., Song, M. M., Reynolds, C. P., & Mossé, Y. P. (2016). Crizotinib synergizes with chemotherapy in preclinical models of neuroblastoma. *Clinical Cancer Research*, 22(4), 948–960.
126. Houghton, P. J., Morton, C. L., Tucker, C., Payne, D., Favours, E., Cole, C., Gorlick, R., Kolb, E. A., Zhang, W., Lock, R., Carol, H., Tajbakhsh, M., Reynolds, C. P., Maris, J. M., Courtright, J., Keir, S. T., Friedman, H. S., Stopford, C., Zeidner, J., Wu, J., Liu, T., Billups, C. A., Khan, J., Ansher, S., Zhang, J., & Smith, M. A. (2007). The pediatric preclinical testing program: description of models and early testing results. *Pediatric Blood & Cancer*, 49(7), 928–940.
127. Townsend, E. C., Murakami, M. A., Christodoulou, A., Christie, A. L., Koster, J., DeSouza, T. A., et al. (2016). The public repository of xenografts enables discovery and randomized phase II-like trials in mice. *Cancer Cell*, 29(4), 574–586.

128. Stewart, E., Federico, S., Karlstrom, A., Shelat, A., Sablauer, A., Pappo, A., & Dyer, M. A. (2016). The childhood solid tumor network: a new resource for the developmental biology and oncology research communities. *Developmental Biology*, *411*(2), 287–293.
129. Murphy, B., Yin, H., Maris, J. M., Kolb, E. A., Gorlick, R., Reynolds, C. P., Kang, M. H., Keir, S. T., Kurmasheva, R. T., Dvorchik, I., Wu, J., Billups, C. A., Boateng, N., Smith, M. A., Lock, R. B., & Houghton, P. J. (2016). Evaluation of alternative in vivo drug screening methodology: a single mouse analysis. *Cancer Research*, *76*(19), 5798–5809.
130. Meehan, T. F., Conte, N., Goldstein, T., Inghirami, G., Murakami, M. A., Brabetz, S., Gu, Z., Wiser, J. A., Dunn, P., Begley, D. A., Krupke, D. M., Bertotti, A., Bruna, A., Brush, M. H., Byrne, A. T., Caldas, C., Christie, A. L., Clark, D. A., Dowst, H., Dry, J. R., Doroshow, J. H., Duchamp, O., Evrard, Y. A., Ferretti, S., Frese, K. K., Goodwin, N. C., Greenawalt, D., Haendel, M. A., Hermans, E., Houghton, P. J., Jonkers, J., Kemper, K., Khor, T. O., Lewis, M. T., Lloyd, K. C. K., Mason, J., Medico, E., Neuhauser, S. B., Olson, J. M., Peeper, D. S., Rueda, O. M., Seong, J. K., Trusolino, L., Vinolo, E., Wechsler-Reya, R. J., Weinstock, D. M., Welm, A., Weroha, S. J., Amant, F., Pfister, S. M., Kool, M., Parkinson, H., Butte, A. J., & Bult, C. J. (2017). PDX-MI: minimal information for patient-derived tumor xenograft models. *Cancer Research*, *77*(21), e62–e66.

Publisher's note Springer Nature remains neutral with regard to jurisdictional claims in published maps and institutional affiliations.